communications biology

Article

https://doi.org/10.1038/s42003-024-07005-8

Prior heat stress increases pathogen susceptibility in the model cnidarian *Exaiptasia diaphana*

Sofia C. Diaz de Villegas[1,2], Erin. M. Borbee[1,2], Peyton Y. Abdelbaki[1] & Lauren E. Fuess[1]

Anthropogenic climate change has significantly altered terrestrial and marine ecosystems globally, often in the form of climate-related events such as thermal anomalies and disease outbreaks. Although the isolated effects of these stressors have been well documented, a growing body of literature suggests that stressors often interact, resulting in complex effects on ecosystems. This includes coral reefs where sequential associations between heat stress and disease have had profound impacts. Here we used the model cnidarian *Exaiptasia diaphana* to investigate mechanisms linking prior heat stress to increased disease susceptibility. We examined anemone pathogen susceptibility and physiology (symbiosis, immunity, and energetics) following recovery from heat stress. We observed significantly increased pathogen susceptibility in anemones previously exposed to heat stress. Notably, prior heat stress reduced anemone energetic reserves (carbohydrate concentration), and activity of multiple immune components. Minimal effects of prior heat stress on symbiont density were observed. Together, results suggest changes in energetic availability might have the strongest effect on pathogen susceptibility and immunity following heat stress. The results presented here provide critical insight regarding the interplay between heat stress recovery and pathogen susceptibility in cnidarians and are an important first step towards understanding temporal associations between these stressors.

Anthropogenic pressure has led to environmental and ecological changes in terrestrial and aquatic ecosystems across the world, often in the form of climate-related events[1,2]. Marine ecosystems, in particular, have been significantly affected by multiple climate-induced stressors, such as ocean warming and disease outbreaks[3–5]. Both of these stressors directly affect organismal physiology through alteration of metabolic function and indirectly affect a variety of ecological processes, such as oxygen availability, nutrient cycling, and ocean circulation[3,6]. As such, ocean warming, specifically marine heat waves, is a leading cause of mass mortality in marine organisms[7–10]. Similarly, increases in the frequency and severity of disease outbreaks pose significant threats to marine ecosystems. Marine taxa are affected by a large diversity of pathogens ranging from viruses and bacteria to fungi and metazoans[11], many of which have triggered significant mortality events in a variety of marine organisms[12–15].

Although the isolated effects of ocean warming, disease outbreaks, and other climate-associated stressors have been well documented within marine ecosystems[3,5], a growing body of literature suggests that these stressors often coincide. Depending on the circumstances and stressors in question, interactions may range from cumulative to synergistic, or even antagonistic in nature[16,17]. Links between heat stress and disease outbreaks are particularly prevalent and have often contributed to extensive marine mortality[18]. Consequently, studies have attempted to improve the understanding of associations between heat stress and disease in marine ecosystems, but most have focused only on the simultaneous synergy between the two stressors[19–21]. However, frequent increases in disease outbreaks following marine heatwaves suggest that these two stressors may more commonly accumulate in a sequential, rather than simultaneous, manner[22–25]. Despite these observations, the mechanisms driving sequential temporal patterns between heat stress and disease are poorly understood and necessitate further investigation.

Coral reef ecosystems present a unique opportunity to investigate sequential associations between heat stress and disease due to the frequency with which these ecosystems are impacted by climate stressors and their well-characterized immune system. These ecosystems are commonly faced with a variety of climate stressors[26], which have resulted in unprecedented declines in coral cover over the past several decades[27,28]. Increasing sea surface temperature (SST), in particular, has exacerbated the frequency and severity of coral decline. Two major drivers of these declines are heat-

[1]Texas State University, San Marcos, TX, USA. [2]These authors contributed equally: Sofia C. Diaz de Villegas, Erin. M. Borbee. e-mail: lfuess@txstate.edu

induced bleaching—loss of endosymbiotic algae[29,30]—and disease[31]. The severity of these declines in recent decades has led to intense focus on the description of cnidarian immunity, which has been revealed to be exceptionally complex and multifunctional, serving in both response to pathogens and stress. Cnidarian responses to pathogens are initiated by a diverse suite of pattern recognition receptors, including Toll-like receptors and NOD-like receptors, which trigger downstream cascades to induce a breadth of effector responses[32,33]. The most prominent of these effector responses are antioxidant production, melanization, and production of antimicrobial compounds[32,33]. The production of antioxidants provides protection against reactive oxygen species generated by both hosts and pathogens during infection and associated immune responses[32–34]. Cnidarians also produce melanin as a result of the prophenoloxidase cascade, which is both directly cytotoxic and has roles in wound healing and pathogen encapsulation[32–34]. Finally, cnidarians are also capable of producing a wide variety of antimicrobial compounds and peptides which can neutralize a number of different pathogenic bacteria[32–34]. Notably, many of these responses, particularly antioxidant production[32,35] and melanization[36], may have roles in heat and other stress-related responses. Consequently, the cnidarian immune system is believed to be a central mechanism contributing to response to most major environmental stressors driving coral decline.

Although isolated heat-induced bleaching events[37–39] and disease outbreaks[40–43] often affect corals, these events have also been frequently observed in close spatial and temporal associations[44–48]. In many cases, coral disease follows bleaching[25], with extensive disease-related mortality often reported in the weeks to months after heat stress[24,49]. Despite these observations, nearly all experimental studies have focused on the synergistic effects of simultaneous heat stress and disease, specifically documenting increases in disease susceptibility when these stressors occur at the same time[50,51]. Synchronous heat stress and disease outbreak events may be linked to heat-induced suppression of immunity[52–56], though other studies have instead demonstrated minimal or positive effects of heat stress on coral immunity[57–59]. It is unclear if similar mechanisms underly sequential associations between heat stress and disease outbreaks.

Sequential heat stress and disease outbreak events may be mediated by several mechanisms. First, heat stress may induce changes in host energetic reserves, which lead to immunosuppression. The loss of symbionts, which typically occurs as a result of heat stress, may severely limit the energetic resources available to the host[60–62]. According to resource allocation theory, organisms must distribute a finite amount of resources amongst diverse biological processes—growth, reproduction, metabolism, immunity, etc.[63–65]. This may involve trade-offs where resources are shifted between competing needs in order to maximize fitness[63–65]. Consequently, a reduction in the total amount of resources may alter the proportions in which resources are distributed, potentially resulting in the suppression of one or more biological processes. As such, immune suppression is one of the most commonly documented energetic trade-offs associated with resource limitation[66,67]. Heat-stress-induced limitations in energetics may exacerbate resource tradeoffs and result in changes to resource allocation, including allocation to host immune responses. Alternatively, immune-energetic trade-offs may also occur in the absence of resource limitation in response to biotic or abiotic pressures: organisms may dynamically shift resources between processes in response to pressing needs caused by environmental stress or other changes in biological condition[68].

Alternatively, dynamic changes in symbiosis during heat stress and associated recovery may contribute to observed links between heat stress and disease outbreaks. Suppression of host immunity by symbionts has been hypothesized as an important mechanism required for the successful establishment and maintenance of symbiotic relationships[69]. Previous laboratory studies have confirmed negative correlations between symbiosis and immunity across several cnidarians[70–73]. However, the dynamics and consequences of immune-symbiosis interplay during the breakdown and re-establishment of symbiosis remain unclear. One possibility is that the rapid repopulation of endosymbionts following heat-induced dysbiosis exacerbates symbiotic immunosuppression, potentially explaining, in part, naturally observed patterns of disease after heat-induced bleaching events.

Here we describe the results of a study aimed at assessing the sequential associations between heat stress and disease outbreaks in cnidarians, with a specific focus on the roles of changes in energetics, symbiont density, and host immunity in these processes. In order to comprehensively address this question, we leveraged the powerful emergent cnidarian model species, *Exaiptasia diaphana* (common name Aiptasia). While tropical scleractinian corals are exceptionally important from an ecological standpoint, their precarious species statuses and inherent experimental limitations complicate the laboratory investigation of complex biological phenomena in these species. In contrast with tropical corals, Aiptasia is easily reared, maintained, and destructively sampled in large amounts without many of the experimental and ethical challenges of working with tropical corals[74]. Aiptasia also maintains symbiotic relationships with endosymbiotic algae of the family Symbiodiniaceae, like tropical corals[75,76]. Finally, Aiptasia is a particularly handy model organism due to the existence of established, genetically identical clonal lines, allowing for control of genetic variation in experimentation[74]. We leveraged the *E. diaphana* model organism to investigate the mechanisms linking heat stress and disease susceptibility in cnidarians. Specifically, we examined host immunity, symbiont density, and energetic reserves following heat stress, as well as the effects of prior heat stress on pathogen susceptibility, in two genetically distinct clonal lines of *E. diaphana*. We document a significant association between prior heat stress and subsequent increased pathogen susceptibility and highlight the potential physiological mechanisms of this association. The results described are an important first step towards understanding temporal links between two of the most significant climate-associated stressors faced by cnidarians.

Results

Mortality

Anemone mortality was significantly greater in anemones exposed to the pathogen (Kaplan–Meier; $N = 184$; $p < 0.001$; Supplementary Fig. 1). Of those anemones exposed to a pathogen, 89% died during the 96-h period, compared to 0% mortality within the placebo group. While there were no significant interactive effects of temperature treatment and clonal line on anemone mortality within the pathogen-exposed anemones subset (Cox Regression; $N = 88$; hazard ratio = 1.32; 95% CI [0.52–3.34]; $p = 0.562$; Supplementary Fig. 2), mortality rate was significantly greater in the heat-stressed anemones relative to the ambient (Cox Regression; $N = 88$; hazard ratio = 2.29; 95% CI [1.11–4.75]; $p = 0.0255$; Fig. 1) and among H2 anemones relative to VWB9 anemones (hazard ratio = 0.197; 95% CI [0.10–0.37]; $p < 0.001$; Fig. 1). When considering just pathogen-exposed anemones, 82% of ambient and 97% of heat stressed individuals died within the 96-h period. Furthermore, 100% of H2 and 82% of VWB9 anemones died.

Symbiont density and energetic reserves

Symbiont density, estimated by mean chlorophyll fluorescence pixel intensity, was significantly affected by temperature treatment, immune challenge, and the interaction of clonal line and both temperature treatment and immune challenge (Table 1). Specifically, symbiont density was higher in previously heat-stressed anemones overall (GLM, $p = 0.0250$), though this effect was more pronounced in H2 anemones. Symbiont density was also higher in H2 than VWB9 anemones, but only in anemones previously exposed to heat stress (Welch's two-sample t-test; $t = 2.51$, $df = 30.066$, $p = 0.01778$. 95% CI [621–6067]; Fig. 2a). No significant interactive effects were observed for carbohydrate concentration, but carbohydrates did vary between clonal lines, temperature treatments, and immune challenge (Table 1, Fig. 2b). Carbohydrate concentration was significantly greater in VWB9 anemones compared to H2 (GLM, $p = 0.0275$), significantly greater in ambient compared to heat-stressed anemones (GLM, $p < 0.01$), and significantly greater in placebo compared to immune challenged individuals (GLM, $p = 0.0441$). Finally, lipid concentration only varied between clonal

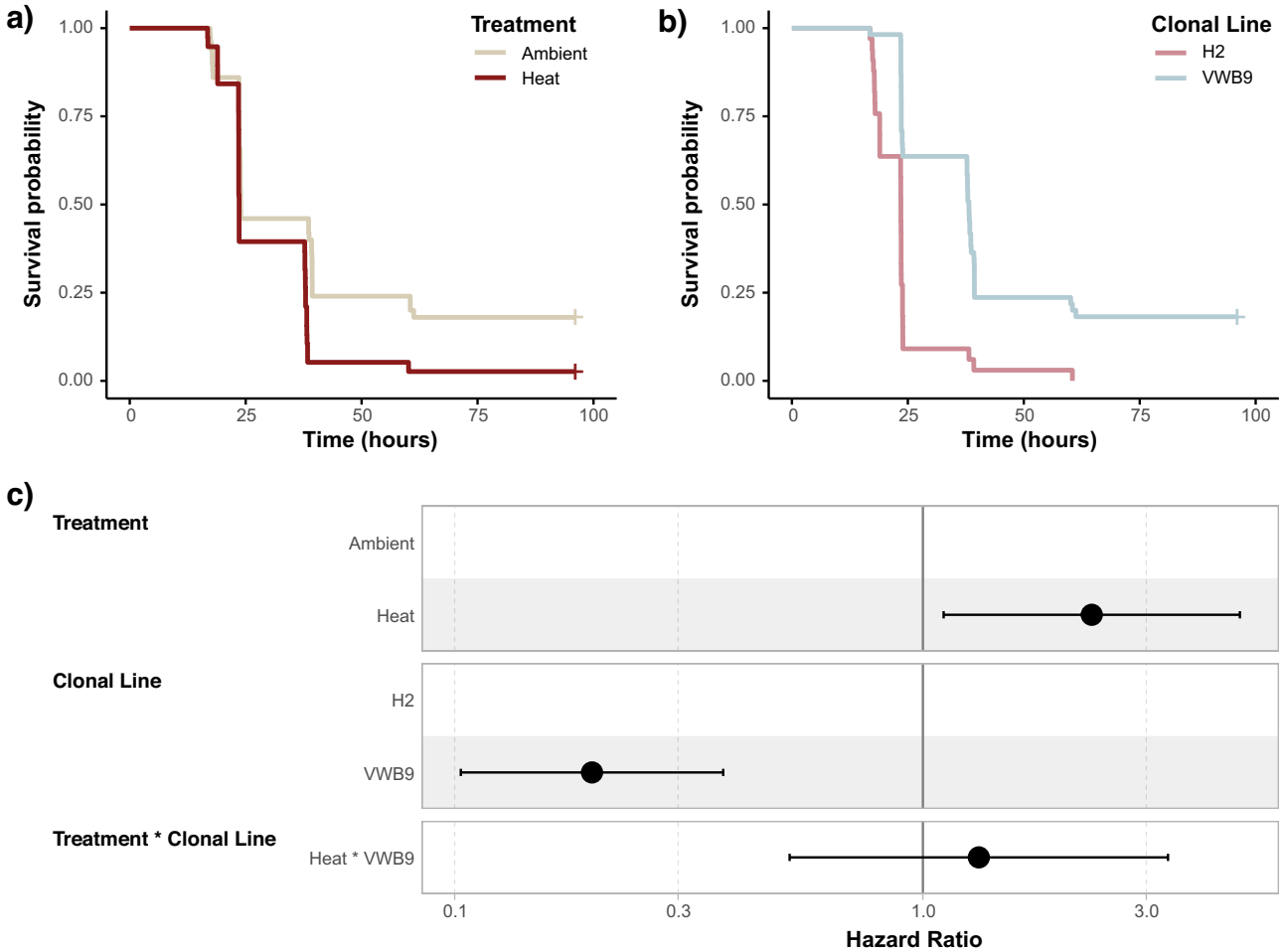

Fig. 1 | Summary of survivorship data from pathogen challenge experiment. **a**, **b** Kaplan–Meier survivorship curves for pathogen exposed anemones split based on comparisons across (**a**) temperature treatment and (**b**) clonal line. **c** Cox proportional hazards models of pathogen exposed anemones compared across temperature treatment and clonal line. The vertical line at 1 indicates the reference to which the second group is compared. The distance from 1 indicates the probability of mortality (i.e., anemones exposed to prior heat stress are approximately twice as susceptible to pathogen exposure than anemones that remained at ambient temperature). Both treatment ($p = 0.0255$) and genotype ($p < 0.001$) had significant impacts on survival. Hazard ratios are displayed for both predictors and the interaction term with 95% confidence intervals.

lines; it was significantly greater in VWB9 anemones compared to H2 (GLM, $p = 0.0151$; Table 1, Fig. 2c).

Immune responses

Immune assays revealed variation in activity/concentration of all parameters measured. Catalase activity ranged from 24.58 to 619.9 mmol H_2O_2 scavenged/min/mg protein, with a mean of 275.6 mmol H_2O_2 scavenged/min/mg protein and a standard deviation of 131.9 mmol H_2O_2 scavenged/min/mg protein. Total phenoloxidase activity ranged from 0.00364 to 0.0308 activity/min/mg protein with an average of 0.0155 activity/min/mg protein and a standard deviation of 0.00610 activity/min/mg protein. Melanin concentration ranged from 0 to 0.00611 mg melanin/mg tissue, with an average of 0.00190 and a standard deviation of 0.00191. Finally, antibacterial activity ranged from −8.68 to 35.7% inhibition of bacterial growth, with a mean of 9.16% and a standard deviation of 10.04%.

The RDA explained significant variation along the first axis of the ordination, RDA1, which explained 18.12% of the total variation ($N = 41$; Fig. 3). Temperature treatment (ANOVA, $p = 0.003$), lipid concentration (ANOVA, $p = 0.003$), and carbohydrate concentration (ANOVA, $p = 0.034$), all explained significant variation in immune responses. Temperature treatment explained significant variation along both the first and second RDA axes (Fig. 3 boxplots; t-test, $p < 0.0001$). However, carbohydrate concentration explained variation mostly along the first RDA axis (Fig. 3 regression bottom-left; Pearson correlation, $p < 0.0001$), while lipid concentration explained variation primarily on the second axis (Fig. 3 regression top-right; Pearson correlation, $p < 0.0001$). The immune variables used to construct the ordination show a strong association with the temperature treatments, with all arrows representing the immune variables pointing towards the group of samples from the ambient treatment.

Linear modeling of the effects of each of our significant predictors on individual immune metrics revealed metric-specific effects (Table 2). Three metrics of immunity (catalase (CAT), total phenoloxidase (TPO), and melanin (MEL)) were significantly lower in heat-treated anemones relative to ambient temperatures (CAT GLM, $p = 0.0129$; TPO GLM, $p = 0.0212$; MEL zero-included binomial, $p < 0.0430$; Fig. 4). Additionally multiple metrics of immunity were positively associated with energetic measurements. Both CAT and MEL were positively associated with carbohydrate concentration (CAT GLM, $p < 0.001$; MEL zero-excluded GLM, $p < 0.001$; Fig. 5), and MEL was also positively associated with lipid concentration (zero-excluded GLM, $p < 0.001$; Fig. 5). Antibacterial activity was not significantly associated with any of the tested predictors.

Table 1 | Symbiont density and energetic reserve linear modeling results

Predictors	Estimates	SE	SEadj	z	p Value
Symbiont density					
(Intercept)	22,082	1864	1896	11.65	<0.001 ***
Treatment	4046	1777	1806	2.241	0.0250*
Clonal line	3557	2005	2042	1.742	0.0815
Immune challenge	4415	1842	1873	2.357	0.0184*
CL : T	−3768	1837	1871	2.014	0.0440*
CL : IC	−5014	1966	2003	2.503	0.0123*
T : IC	594.9	1376	1392	0.427	0.6691
Carbohydrate concentration					
(Intercept)	0.09532	0.008953	0.009078	10.50	<0.001 ***
Treatment	−0.02984	0.01163	0.01178	2.535	0.0113*
Clonal Line	0.02122	0.009505	0.009628	2.204	0.0275*
Immune Challenge	0.01879	0.009212	0.009333	2.013	0.0441*
CL : T	−0.004741	0.01165	0.01174	0.404	0.6864
T : IC	−0.003919	0.01062	0.01071	0.366	0.7144
Lipid concentration					
(Intercept)	0.3804	0.03519	0.03565	10.67	<0.001 ***
Treatment	0.01668	0.03345	0.03372	0.495	0.6208*
Clonal line	0.1036	0.04201	0.04260	2.431	0.0151*

Best-fit linear models for symbiont density, carbohydrate concentration, and lipid concentration when including temperature treatment, clonal line, and immune challenge as predictors. Asterisks (*) represent significant *p*-value ($\alpha = 0.05$; * $p < 0.05$, ** $p < 0.01$, *** $p < 0.001$). *CL* clonal line, *IC* immune challenge, *T* treatment

Discussion

As anthropogenic climate change worsens, marine ecosystems are faced with a multitude of stressors that may form complex associations with each other[3,5,17]. However, empirical study of interactive stressors, particularly those occurring asynchronously, has been limited, leaving many questions regarding the nature and mechanisms of associations amongst stressors[77]. Cnidarians, which face a diversity of climate-related stressors[21,32,78,79], provide a relevant model to investigate the effects of multiple stressors (both interactive and sequential) on marine species. Here we conducted one of the first experimental studies investigating the consequences of prior heat stress on subsequent pathogen susceptibility. Our results support a long-held theory[80] that previous heat stress increases later pathogen susceptibility and provide important new insight regarding these patterns. Specifically, we highlight changes in host cnidarian immunity following heat stress which may be driven by shifting resource allocation and likely contribute to observed patterns of differential pathogen susceptibility. These results are an essential first step toward understanding the cellular mechanisms that contribute to associations between sequential stressors.

Mortality differs across temperature treatments and clonal lines

Anemones exposed to heat stress were approximately twice as susceptible to pathogen exposure after two weeks of recovery compared to temperature control individuals. This result is in agreement with documented increases in disease and disease-related mortality following coral bleaching in the wild[24,45,49,81]. Notably, while previous laboratory experiments have documented impacts of simultaneous heat stress and pathogen exposure[50,52,55,56,82], ours is the first to document the prolonged consequences of heat stress on pathogen susceptibility, more accurately representing observed environmental patterns in nature. Future studies combining our approach with emergent experimental disease techniques[83,84] will allow for more broadscale applications to complex cnidarian and marine disease systems.

We also observed significant genotypic differences in mortality. Anemones from the VWB9 clonal line were less susceptible to pathogen-induced mortality than H2. Both clonal lines originate from similar geographic regions and host the same species of algal endosymbiont (*Brevolium minutum*)[85], suggesting some degree of genetic, epigenetic, or plastic variation contributes to observed physiological differences between the lines. While intraspecific variation in cnidarian disease resistance has been linked to genetic variation in the wild[86,87], there is a lack of studies investigating this variation in laboratory settings[88]. Similarly, most experimental studies investigating pathogen dynamics in Aiptasia use only a single clonal line[50,89–91]. Our findings suggest that the inclusion of genetic variation in cnidarian studies, including those involving *E. diaphana*, may provide increased insight regarding the roles of genetic variability in contributing to stress resistance or susceptibility.

Mechanisms of differential mortality: roles of symbiont density and energetic reserves

Beyond documenting differences in mortality as a result of environmental and genetic factors, we employed an integrative approach to investigate the underlying mechanisms driving these differences. Given the well-known contributions of symbiont density and energetic reserves to cnidarian host immunity and pathogen susceptibility[70,92,93], as well as the documented effects of heat stress on these metrics[62,94–97], we specifically sought to examine differences in symbiont density and energetic reserves between temperature treatments. Contrary to expected results, symbiont density was higher in previously heat-stressed individuals following two weeks of recovery, potentially due to *E. diaphana*'s capacity for exceptionally rapid recovery from dysbiosis[98]. This effect did vary across genotypes; H2 anemones had significantly higher symbiont density than VWB9 anemones in the prior heat treatment group only.

Our results suggest that the two-week recovery between heat stress and pathogen challenge was likely ample time for anemones to recover from any dysbiosis and even overcompensate in some clonal lines. Elevated symbiont densities in previously heat-stressed individuals may be the result of unregulated symbiont growth during recovery. As negative associations have frequently been observed between symbiont density and immunity in other cnidarians[69–71], the unchecked growth of symbionts during recovery may have contributed to differential mortality. Consistent with this hypothesis, H2 anemones, which were more susceptible to pathogen exposure, also had consistently higher symbiont densities. In contrast to symbiont density, carbohydrate concentration was reduced in those anemones that had undergone previous heat stress. We also observed differences in energetic reserves between clonal lines; VWB9 had higher concentrations of both carbohydrates and lipids than more susceptible H2 anemones. Finally, immune challenged anemones also had reduced carbohydrate concentrations, likely indicative of a reallocation of resources to immune responses as has been described in other systems[66]. Combined, these results suggest that energetic reserves are necessary for responding to pathogen challenge, and reduced energetic reserves may have a more significant impact on pathogen susceptibility than variation in symbiont density at this stage of bleaching recovery (i.e., 2 weeks). Time series and finer-scale approaches leveraging metabolomic or carbon-flux modeling are needed to determine the potentially shifting effects of symbiont density and energetic reserves on host–pathogen susceptibility over the course of bleaching recovery.

Mechanisms of differential mortality: roles of host immunity

Next, we focused on the potential roles of shifts in immunological activity that might contribute to observed patterns of mortality. When considering immunity using multivariate statistics, we saw significant effects of temperature, carbohydrate, and lipid concentration on immune response. Particularly, we saw an indication of immune suppression in anemones that had undergone prior heat stress. Examination of the effects of heat stress on

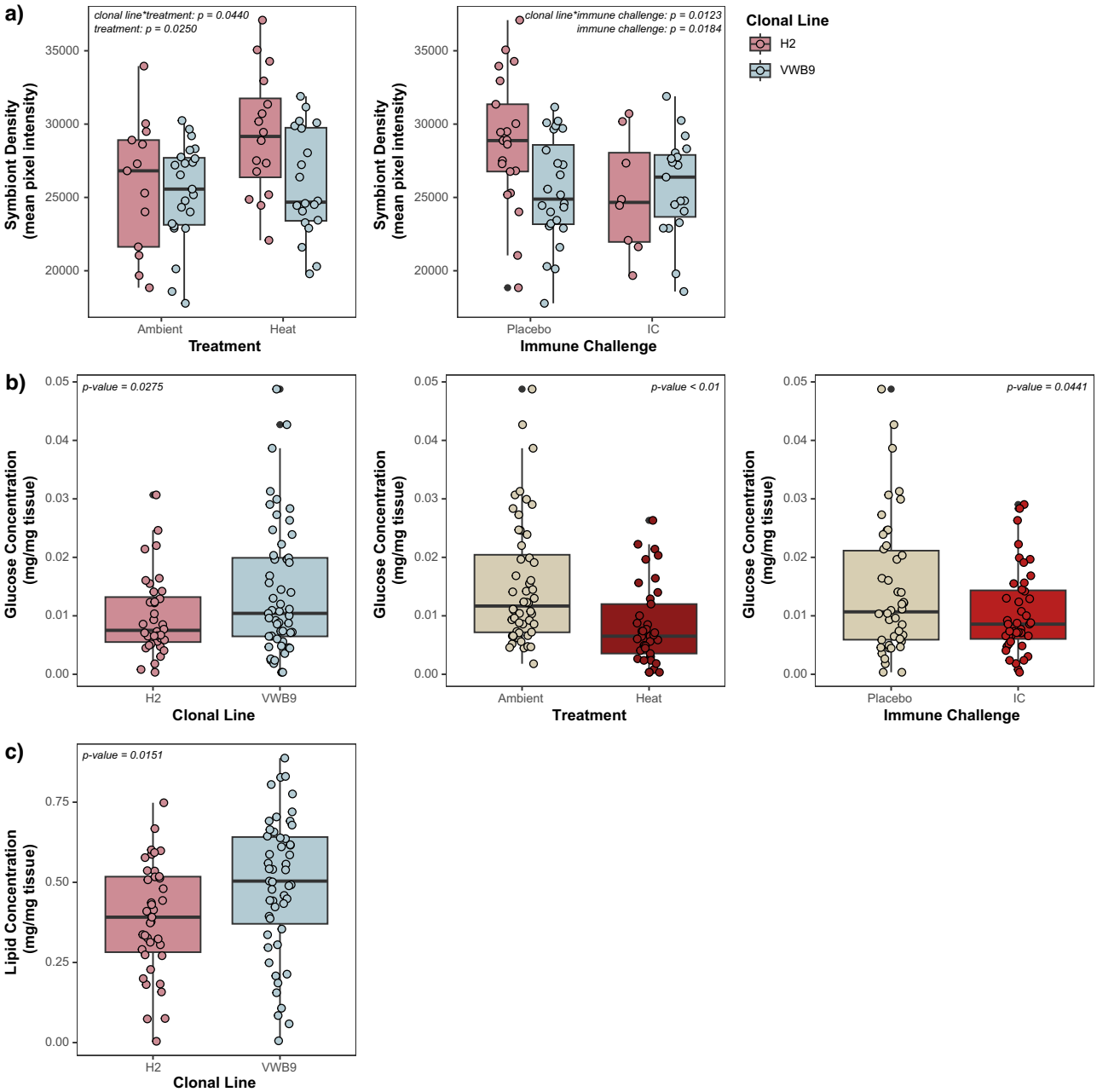

Fig. 2 | Effects of clonal line and prior heat treatment on symbiont density and energetic reserves. Box plots displaying effects of identified significant predictors on **a** symbiont density, **b** carbohydrate concentration, and **c** lipid concentration. Raw data values are represented by overlaid points; boxes and points are colored based on factors of interest. Significance (*p values*) for identified significant predictors and relevant interaction terms reported. IC immune challenge.

individual immune parameters revealed strong suppression of catalase activity, total phenoloxidase activity, and melanin concentration. While numerous studies have evidenced the short-term effects of heat stress (days–weeks) on cnidarian host immunity[36,53,82,99], the long-term effects of heat stress (months – years) on immune activity are not well documented[100,101]. Many studies have noted heat-induced activation of a variety of immune parameters, including antioxidant (e.g., catalase) and phenoloxidase enzymes[53,99,100], though some studies report minimal or negative impacts of heat on immunity[57–59]. Positive associations between heat stress and immune responses during simultaneous stressors may be driven by overlap between response mechanisms; some heat stress biomarkers (i.e., HSP70) are known to activate immune pathways such as melanin synthesis[102,103]. In contrast to the synergy that often occurs between heat stress and immune activation during simultaneous stressors, we document a pronounced reduction in immunity (catalase, phenoloxidase, melanin) after 2 weeks of recovery from heat stress. Our approach suggests significant immune reduction occurs during recovery, potentially with lasting effects, though the exact timing is unclear. Frequent, repeated sampling during heat stress and recovery will improve understanding of the prolonged effects of increasing SSTs on cnidarian immunity.

Investigating the role of energetic immunosuppression and the importance of resource allocation

One potential hypothesis to explain observed associations between heat stress and immunity is that changes in resource allocation as a result of resource limitations during dysbiosis may result in immune suppression. The strongest support for this hypothesis comes from our analyses involving carbohydrate concentrations, which were significantly reduced as a result of prior heat stress. Additionally, carbohydrate concentration was strongly positively associated with both catalase activity and melanin

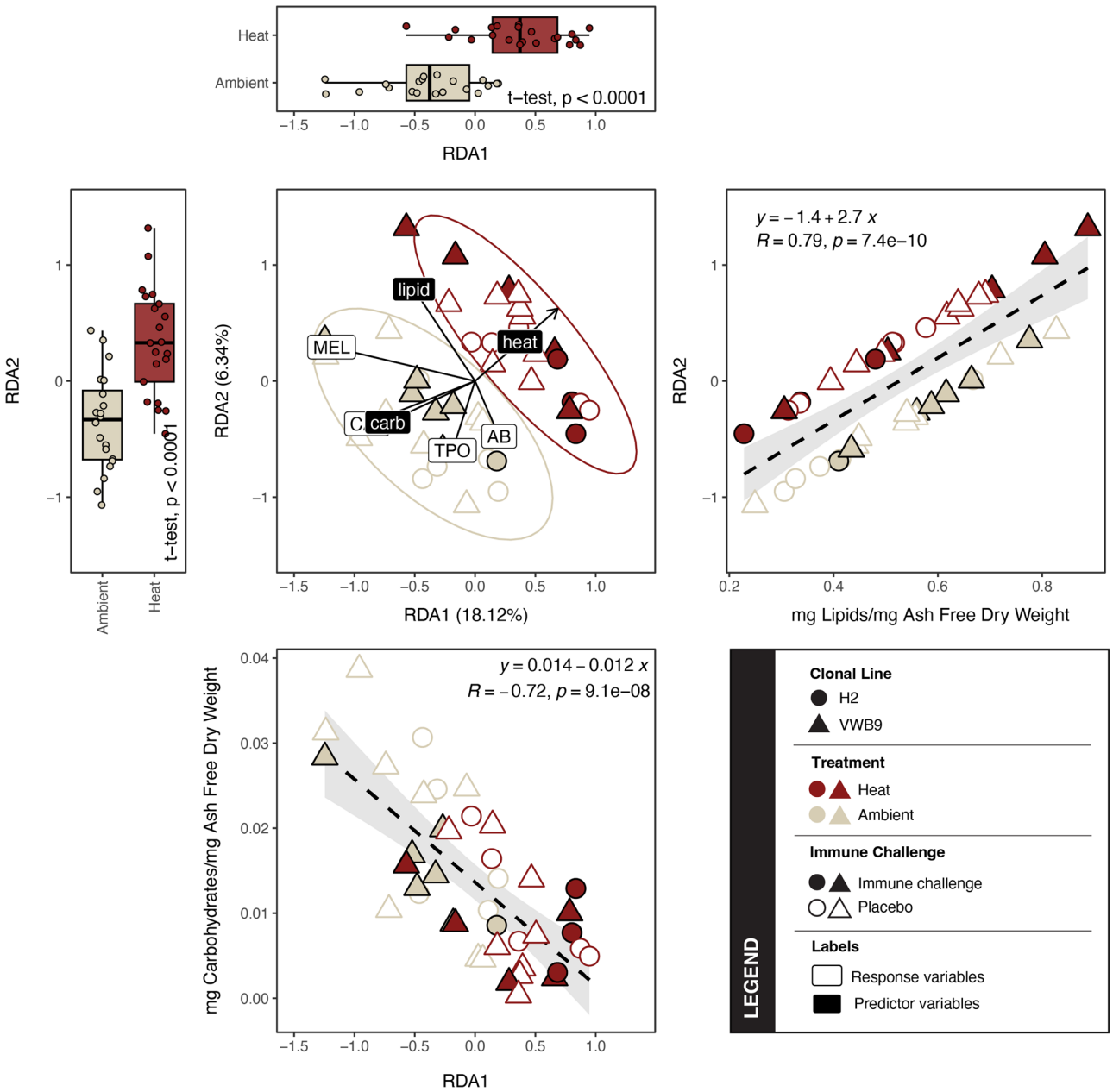

Fig. 3 | Multivariate analysis of significant predictors of immunological variation. RDA plot (center) showing significant predictors (black labels) for explaining variation in immunity. Data points represent individual samples, and ordination was constructed using distances generated from immune parameters. The color indicates temperature treatment, the shape indicates clonal line and open shape/filled shape indicates immune challenge. Black labels represent predictor variables, and white labels represent response variables. Arrows represent the strength and directionality of each variable in multi-variate space. Boxplots on the top and far left indicate the distribution of heat and ambient points along the first and second axes to demonstrate significant variation explained by temperature treatment in each direction. Regressions on the bottom and far right show the correlation between carbohydrates and lipids on the first and second axes, respectively, to demonstrate a significant explanation of variation by those variables on each axis. *MEL* melanin, *CAT* catalase, *TPO* total phenoloxidase, *AB* antibacterial activity.

concentration, both of which were more active/abundant in samples from the ambient group. Combined, these data suggest that reductions in carbohydrate concentrations due to prior heat stress have direct effects on immunity; as energetic reserves decrease in response to prior heat stress, certain immune responses appear suppressed. These findings are consistent with the synthesis of previous results. Heat stress both causes the reallocation of host energetic reserves to stress responses and often impacts overall energetic reserves through the reduction in symbiont density, which provides nutritional resources to hosts[97,104–109]. This loss of energetic resources likely results in a decrease in the total energy available to allocate to immune defenses, consistent with resource allocation theory[66,67,110].

Associations between lipid and melanin concentrations further support the notion that changes in energy affect host immunity. Melanin concentration was also significantly positively correlated to lipid concentration, which was not affected by prior heat stress. Reduced effects of prior heat stress on lipids compared to carbohydrates are consistent with previous findings; stored carbohydrates, rather than lipids, are preferentially used as an energy source by hosts during bleaching recovery in other cnidarians[97]. The association between melanin and lipids, which were relatively unaffected by prior heat stress, suggests that melanin production potentially draws resources from both lipids and carbohydrate sources. The use of both lipids and carbohydrates to fuel melanin production could account

Table 2 | Immune metric linear modeling results

Predictors	Estimates	SE	SEadj	z	*p* Value
Catalase					
(Intercept)	15.68	0.901	0.913	17.18	<0.001***
Treatment	−3.12	1.24	1.25	2.49	0.0129*
Carbs	141.9	36.76	37.01	3.80	<0.001***
Lipid	0.431	1.47	1.48	0.290	0.772
Lipids : Treatment	0.775	2.10	2.11	0.367	0.714
Carbs : Treatment	13.62	45.99	45.42	0.293	0.769
Antibacterial activity					
(Intercept)	12.58	5.50	5.55	2.27	0.0235*
Treatment	−0.642	1.699	1.717	0.374	0.708
Carbs	79.64	121.4	122.4	0.651	0.515
Lipids	−8.11	9.17	9.26	0.876	0.381
Total phenoloxidase					
(Intercept)	0.0164	0.0016	0.00117	13.98	<0.001***
Treatment	−0.00323	0.00138	0.00140	2.304	0.0212*
Carbs	0.0210	0.0514	0.0519	0.405	0.686
Melanin†					
Predictors	X^2		**DF**		***p* Value**
Treatment	4.097		1		0.0430*
Carbs	0.3801		1		0.5376
Lipids	1.677		1		0.1960
0 s removed Melanin†					
Predictors	**Estimates**	**SE**	***t***		***p* Value**
(Intercept)	−1.98E−03	8.98E−04	−2.20		0.0321*
Treatment	−1.81E−04	4.62E−04	−0.392		0.697
Carbs	0.0706	0.0215	3.28		<0.001***
Lipids	6.64E−03	1.38E−3	4.68		<0.001***

Best-fit linear models for each immune parameter when including temperature treatment, clonal line, immune challenge, and lipids as predictors.
†models that did not undergo model dredging and averaging.
Asterisks (*) represent significant *p*-value ($\alpha = 0.05$; * $p < 0.05$, ** $p < 0.01$, *** $p < 0.001$).

for comparatively reduced impacts of heat on this metric compared to other immune parameters like catalase. Together, our results suggest that changes in total energetic resources directly impact host immunity in the aftermath of heat stress.

Investigating the role of symbiotic immunosuppression

A second commonly cited potential mechanism linking sequential heat stress and disease outbreaks is immunosuppression, linked to rapid symbiont population regrowth. While our observation of higher symbiont density in groups more susceptible to pathogen challenge (i.e., previously heat stressed and H2 anemones) is consistent with this hypothesis, we did not document any significant associations between symbiont density and our measured metrics of immunity. Two potential explanations exist: (1) we measured a limited suite of immune metrics; symbiont-induced immune suppression may have effects on unmeasured metrics, or (2) indirect or time-lagged effects of changing symbiont densities may be influencing observed patterns of differential mortality. Specifically, rapid and excessive symbiont proliferation (evidenced by higher symbiont densities in heat-treated anemones) may have had significant prolonged effects on host immunity that were not detected at the time of sampling (i.e., time-lagged effects). Future studies incorporating more immune parameters and time-series approaches to sampling may be used to test these hypotheses.

Conclusion and future directions

Multiple stressors are a common consequence of anthropogenic climate change and can have pervasive effects on a variety of marine ecosystems[17]. As such, an improved understanding of organismal responses to climate-induced stressors is imperative to the conservation of these ecosystems. Here we detail one of the first studies to link prior heat stress and increased disease susceptibility in a marine species. Our study establishes the ability to reproduce heat stress and disease associations under laboratory conditions using a tractable model organism, allowing for more nuanced and robust investigations of ecologically relevant phenomena. Using this experimental approach, we were able to demonstrate the prolonged effects of prior heat stress on host immunity, which may contribute to observed increased pathogen-induced mortality following recovery from heat stress. Furthermore, our results implicate changes in resource availability as a potential mechanism of heat-induced immunosuppression. Further studies incorporating time series approaches will be necessary to fully disentangle the observed patterns and associated mechanisms and assess their broad applicability to marine systems. Specifically, future work should aim to sample across multiple timepoints from the onset of bleaching through acute and long-term recovery to determine the effects of dynamic changes in symbiont density and energetic reserves on host immunity and pathogen susceptibility. This, coupled with more nuanced approaches such as fine-scale metabolomics and transcriptomics, should provide a clearer picture of the nuances of changing resource allocation, symbiont density, and immunity which link prior heat stress to increased pathogen susceptibility in cnidarians. In summary, our results provide an important starting point for understanding the links between heat stress and disease that will aid in the conservation of marine species, especially cnidarians, in the face of a changing climate. Most importantly, they generate testable hypotheses that will be invaluable in better understanding the effects of multiple stressors on diverse species and ecosystem functions.

Methods

Experimental design

Anemones were obtained from laboratory-maintained clonal lines of symbiotic *E. diaphana* (VWB9 and H2; V. Weis). Anemones from each clonal line were randomly assigned to one of four possible treatment combinations: ambient temperature and placebo, heat stress and placebo, ambient temperature and immune challenge, or heat stress and immune challenge (Table 3). Individuals were transferred accordingly into sterile, lidded 6-well culture plates filled with 10 mL of filter-sterile artificial seawater (FASW). Each well contained a single anemone and plates were distributed such that each treatment combination had 30 plates. Plates assigned to ambient temperature treatment were maintained in a single temperature-controlled incubator (Percival Scientific; Model AL-41L4) at 27 °C for the duration of the experiment. Plates assigned to heat stress treatment were randomly divided between two separate temperature-controlled incubators (VWR; Model 2005, VWR; Model 3734). Prior to the start of the experiment, all individuals were acclimated to well plates for four days at 27 °C in their respective incubators. Anemone mortality throughout the duration of the experiment was largely limited to this acclimatization period (98% of mortality), likely an effect of the transition from larger containers to individual wells. Final sample sizes, accounting for acclimatization mortality, are found in Table 4. Throughout the entire experiment, anemones in all three incubators were maintained under the same light conditions (12 h:12 h light: dark cycles with approximately 40–60 μmol m^{-2} PAR) and were fed bi-weekly (*Artemia nauplii)* and subsequent water changes until the point of immune challenge. Plate locations were randomized within and between incubators at the time of water changes, as appropriate.

Experimental heat stress and pathogen challenge

Heat-stressed anemones were exposed to a temperature profile that consisted of a 7-day ramping period wherein temperatures were raised 1 °C per day to a final temperature of 34 °C which was maintained for 5 days before

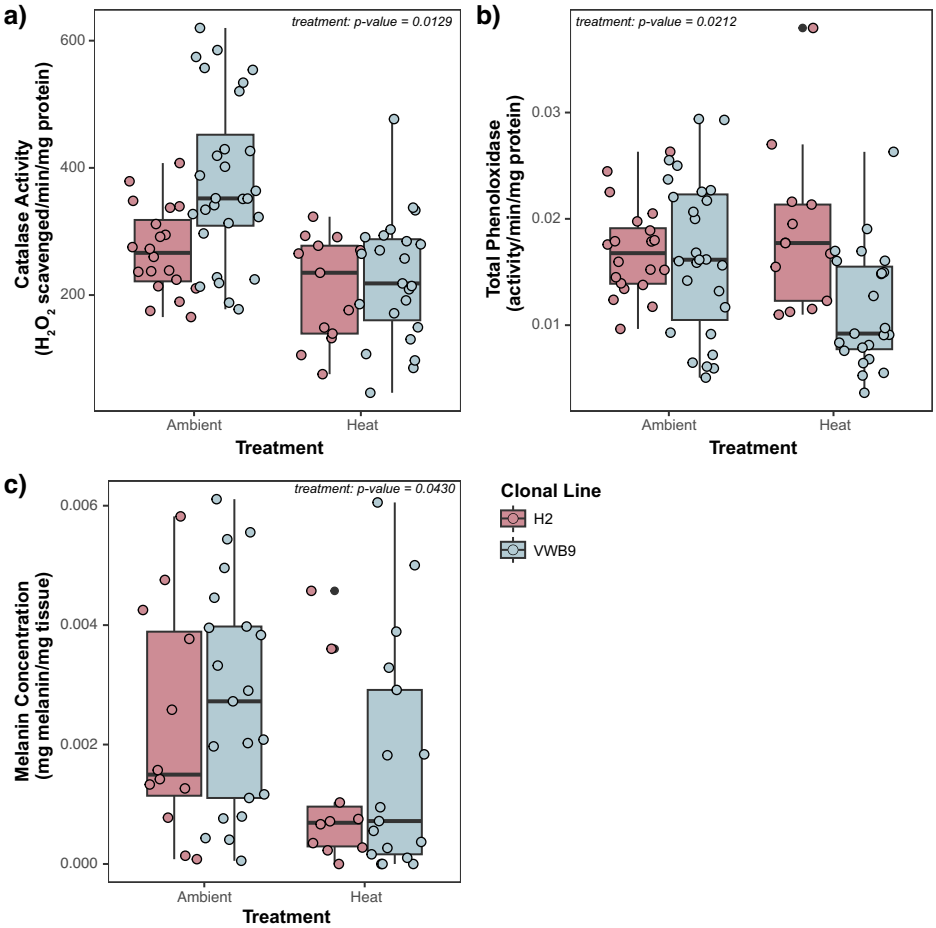

Fig. 4 | Variation in individual immune metrics as a result of prior heat treatment. Box plot displaying differences in **a** catalase activity, **b** total phenoloxidase activity, and **c** melanin concentration as a result of temperature treatment, divided by a clonal line. Raw data values are represented by overlaid points; boxes and points are colored based on clonal lines. Significance (*p* values) for treatment is reported.

Table 3 | Initial sample sizes

	VWB9		H2	
	Ambient	Heat	Ambient	Heat
Placebo	86	86	86	86
Immune challenge	86	86	86	86

an immediate return to ambient temperatures (27 °C) on day six. The chosen protocol was developed based on previous studies that used 34 °C as a target temperature[50,111,112] and pilot data which demonstrated this regime induced significant bleaching (measured as a decline in pixel intensity in chlorophyll fluorescence images) with limited mortality (Supplementary Table 1). This approach was employed to mimic a sublethal bleaching event from which individuals recover so as to test our hypotheses regarding the impact of the re-establishment of symbiosis on host immunity. During the experiment, bleaching was confirmed by visual assessment of anemone color and was found to be consistent with the expected timeline. Following heat stress, anemones were immediately returned to 27 °C and allowed to recover for two weeks. At the conclusion of this recovery period, surviving anemones from both temperature treatments were inoculated with either a pathogen or a placebo (FASW) by plate, according to a priori assignments. Pathogen exposure was conducted using the known coral pathogen *Vibrio coralliilyticus* BAA 450[113] at a predetermined dosage of 1×10^8 CFU mL^{-1}[50]. Final bacterial concentrations were confirmed with serial dilutions and plating. Following exposure, a subset of anemones was monitored for survivorship (Table 4): mortality data was collected every 2 h for the first 24 h and then daily for the remainder of the experiment (96 h post-immune challenge), at which point 89% of exposed anemones had died. Individuals were considered dead when they exhibited tissue degradation characterized by loss of tentacle and overall polyp shape for more than 24 h.

Sample collection and processing

Twelve hours after inoculation, a second subset of randomly selected anemones was sampled for the assessment of symbiont density, immune activity, and energetic reserves (Table 4). Anemones were anesthetized in 10 mL of $MgCl_2$ (0.37 M) prior to sampling. First, we excised a single tentacle for estimates of symbiont density as described below. Tentacles were processed and mounted on microscope slides following standard protocols[98]. Following tentacle excision, the remaining anemone was halved using a sterile razor blade; one half was flash-frozen for the immune and energetic assays described herein. The other half was preserved for future analyses. Anemones were homogenized following an existing protocol with minor modifications[114]. Frozen tissue samples were homogenized with 3 mm glass beads in 1.5 mL of 100 mM Tris + 0.05 M DTT buffer (pH 7.8) for 1 minute at 5 m s^{-1} using a bead mill (Fisherbrand). For each sample, a 200 µL aliquot of homogenate was transferred into a separate microcentrifuge tube and stored at −20 °C for melanin assays. The remaining homogenate for each sample was then transferred into a new 2 mL microcentrifuge tube and centrifuged at 2250×*g* at 4 °C for 5 min. Resulting supernatants were aliquoted accordingly for each set of assays (protein, lipid, carbohydrates, ash-free dry weight) and stored at −80 °C (protein fraction) or −20 °C (all other fractions) prior to downstream analyses.

Symbiont density estimation

Mounted tentacles were imaged using brightfield and fluorescence microscopy on the Cytation1 Cell Imaging Multimode Reader (Biotek). The

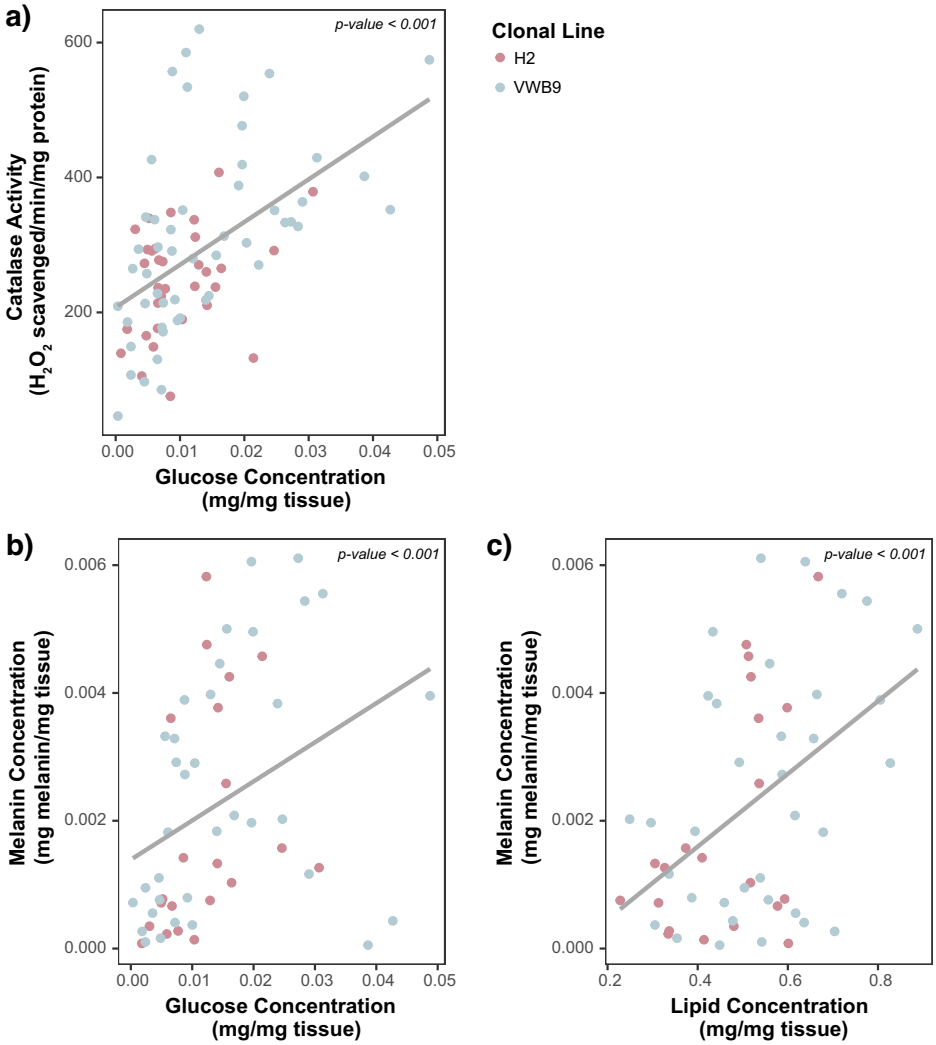

Fig. 5 | Correlations between individual immune metrics and energetic reserves. Best-fit linear models of the association between individual immune assays and energetic metrics: **a** catalase activity and carbohydrate concentration, **b** melanin concentration and carbohydrate concentration, and **c** melanin concentration and lipid concentration. Points represent individual samples color-coded by clonal lines. Trendlines represent linear models of association between immune and energetic metrics (independent of clonal lines). Significance (*p* values) for associations are reported.

Table 4 | Final sample sizes split by analysis

	VWB9		H2	
	Ambient	Heat	Ambient	Heat
Survivorship				
Placebo	30	26	19	21
Immune challenge	30	25	20	13
Physiology				
Placebo	14	13	12	11
Immune challenge	17	12	11	10

approximate tentacle area was determined via brightfield microscopy. Symbiont autofluorescence was visualized using a chlorophyll fluorescent filter (Agilent; EX 445/45 nm, EM 685/40 nm). Brightfield and fluorescent images of each tentacle were combined to standardize fluorescence by tentacle area. The average pixel intensity of the chlorophyll fluorescence within each standardized tentacle area was used as a proxy for symbiont density.

Immune assays

Cnidarian immunity was measured using a suite of standardized immune assays originally developed for scleractinian corals[115,116] and adapted for use in *E. diaphana*. We measured responses related to three major innate immune pathways: antioxidant, phenoloxidase, and antibacterial pathways. All immune assays were run in triplicate on separate 96-well plates and measured using the Cytation1 Cell Imaging Multimode Reader and Gen5 Software (Biotek). Negative controls for all assays were 100 mM Tris + 0.05 mM DTT buffer (homogenization buffer). All enzymatic immune assays were standardized by protein concentration using established protocols for Red660 colorimetric assays[115,116], while melanin concentration was standardized by desiccated tissue weight.

Catalase activity was measured using established protocols[115,116]. Briefly, 5 µL of protein sample were combined with 45 µL of 50 mM PBS (7.0 pH) and 75 µL of 25 mM H_2O_2 in a UV 96-well plate. Immediately following the addition of H_2O_2, absorbance at 240 nm was read every 45 s for 15 min. Catalase activity was determined from the steepest portion of the reaction curve. The total hydrogen peroxide scavenged during this period was calculated using a standard curve of H_2O_2. Final catalase activity is reported as H_2O_2 scavenged per minute per mg of protein.

We quantified the phenoloxidase cascade using both total phenoloxidase activity (enzymatic activity of trypsin-activated prophenoloxidase + phenoloxidase) and melanin concentration (see next section). Total phenoloxidase activity was estimated using modifications to existing protocols[116]. Briefly, 20 µL of protein sample were combined with 20 µL of 50 mM PBS (7.0 pH) and 25 µL of 0.1 mg mL^{-1} trypsin. Samples were then incubated on ice for 30 min to allow for cleavage of prophenoloxidase into phenoloxidase. We then measured total potential phenoloxidase activity (i.e., the activity of any existing phenoloxidase in the sample + activity of

prophenoloxidase activated during trypsin incubation). Following incubation, 30 µL of 10 mM L-DOPA were added to each well to initiate melanin synthesis. Absorbance at 490 nm was read every 10 min for 4 h. Total phenoloxidase activity was calculated from the steepest portion of the reaction curve and standardized to sample protein concentration.

Melanin tissue concentration was estimated using reserved homogenate samples following established protocols[115,116]. Briefly, samples were desiccated in a speed vac (Eppendorf Concentrator Plus) for a minimum of 12 h. Following desiccation, samples were weighed to obtain total desiccated tissue weight. Then, 1.0 mm glass beads (Sigma Aldrich) and 400 µL of 10 M NaOH were added to each sample. Samples were vortexed for 20 s and stored in the dark for 48 h. During this incubation, samples were vortexed briefly at 36 and 48 h. At the end of this period, samples were centrifuged at 183×*g* for 10 min at room temperature. A melanin standard, processed identically to samples, was used to create a standard curve. To measure melanin concentration, 40 µL of the resulting supernatant from samples or melanin standard dilutions were transferred to half-volume UV 96-well plates. Absorbance was measured at 490 nm and converted to melanin concentration using the standard curve. All melanin values were standardized by desiccated tissue weight.

Antibacterial activity was quantified by measuring bacterial growth rates of *V. coralliilyticus* in the presence of protein extracts generated from host tissue. Antibacterial activity against *V. coralliilyticus* BAA 450 was calculated using established protocols[115]. Prior to the assay, samples were diluted to a standardized protein concentration. To initiate the reaction, 60 µL of sample (or buffer control) was combined with 140 µL of *V. coralliilyticus* diluted to an OD 600 of 0.2. Absorbance was read at 600 nm every 10 min for 6 h to generate bacterial growth curves. Percent inhibition of bacterial growth was calculated by comparing the sample growth rate to the growth rate of buffer controls from the steepest portion of the curve.

Energetic assays

Total lipids and total carbohydrates assays were used to determine approximate host energetic budget. Lipids and carbohydrates are commonly used proxies for energetic budgets in multiple cnidarian species[117]. Total lipid and total carbohydrate assays were run in triplicate and duplicate, respectively, and measured in separate 96-well plates using the Cytation1 Cell Imaging Multimode Reader and Gen5 Software (Biotek). Tris + DTT buffer was used as a negative control for both assays.

Sample ash-free dry weight was calculated to standardize both lipid and carbohydrate assays using modifications from previous methods[118]. All samples were weighed using an analytical scale. Briefly, a recorded volume of sample was added to tared aluminum boats and dried at 60 °C in a drying oven for 48 h. Samples were removed from the drying oven and weighed before combusting at 500 °C for 4 h in a furnace box. Following combustion, samples were weighed one final time. Ash-free dry weight was calculated as the average difference between the dry weights and ash weights of each sample and standardized to 125 µL volume.

Lipid concentrations were estimated using a total lipid assay following established protocols[119]. Samples were dried for 5 h at room temperature in a speed vac and then combined with 500 µL 2:1 chloroform: methanol solution and 100 µL of 0.05 M NaCl. Tubes were vortexed for 20 s before 2-h incubation on a shaking incubator at 200 RPM, with brief vortexing approximately every 30 min. At the end of this period, samples were centrifuged at 1650×*g* for 10 min at room temperature. One hundred microliters from the bottom organic layer of each sample were transferred in triplicate to a 96-well PCR plate. A serial dilution of corn oil standard dissolved in chloroform was also plated for the creation of a standard curve. Next, 50 µL of methanol was added to each well. The plate was incubated in a 70 °C water bath for at least 15 min to evaporate the solvent, after which 150 µL of 18 M sulfuric acid (H_2SO_4) was added to each well. The plate was then covered and incubated at 90 °C for 20 min and cooled to 4 °C. Following this incubation, the plate was vortexed, and 75 µL of each sample and standard were transferred into a new 96-well microplate. Following baseline absorbance measurement at 540 nm, 34.5 µL of mg mL^{-1} vanillin in 17% phosphoric acid was then added to each well. After a 5-min dark incubation period, absorbance values were read again at 540 nm and subtracted from the initial reads. Average differences in absorbance values were converted to lipid concentration using the standard curve and standardized by initial sample volume and ash-free dry weight.

Carbohydrate concentrations were estimated following established protocols[120]. Fifty microliters of either sample or glucose standard were plated in duplicate on a 96-well microplate. Next, 150 µL of 18 M H_2SO_4 was added to each well, followed immediately by 30 µL of 5% phenol. Plates were incubated (uncovered) in a hot water bath for 5 min at 80 °C and allowed to cool for 15–20 min. Absorbance values were measured at 485 and 750 nm. Total carbohydrates were calculated by converting the average difference between 750 and 485 nm absorbance values to glucose concentrations using a standard curve. Carbohydrate values were standardized to tissue weight using ash-free dry weight.

Statistics and reproducibility

All statistical analyses were performed using R Version 4.4.0[121]. General sample sizes for each analysis are reported in Table 4; replicates are defined as individual anemones. Prior to modeling, sample outliers were identified using the Rosner test from the EnvStats package (v2.8.1[122]) and removed. Shapiro–Wilke and Bartlett tests were used to confirm the assumptions of normal distribution and equal variances, respectively. Data from some assays failed to meet assumptions necessary for parametric testing, even following transformation, necessitating the use of non-parametric analyses.

Survivorship data from our first subset of anemones were used to assess the effects of pathogen exposure, heat stress, and clonal line on mortality. First, we tested for a significant effect of pathogen exposure on mortality using a Kaplan-Meier analysis (Survival ~ pathogen challenge; $N = 184$; survival package v3.5.5[123]). Mortality data within pathogen-exposed groups were then statistically evaluated using standard approaches for survival analyses, specifically a Cox proportional hazard model, which both allows for censorship of individuals (i.e., those that did not die) and incorporates data regarding the rate of mortality[124,125]. We investigated the interactive effects of heat stress and clonal line on mortality within the subset of pathogen-exposed anemones only (Survival ~ temperature * clonal line; $N = 88$).

A second subset of anemones reserved for assessment of symbiont density, energetic reserves, and immune activity, was used to investigate hypotheses related to mechanisms of differential mortality. To start, we assessed the effects of categorical factors of interest (clonal line, temperature treatment, immune challenge) on symbiont density and energetic reserves using linear modeling approaches (GLMs). Carbohydrate concentration was square root transformed prior to analyses to meet assumptions of normality. Global models with all possible additive and interactive variables were analyzed. All models were dredged and ranked via AICc using the MuMIn package (v1.47.5)[126], where applicable. Models with delta AICc values less than or equal to 2 were averaged to determine the best-fit models for each immune parameter.

To investigate the impact of our independent variables (temperature, pathogen exposure, and clonal line) and covariates (symbiont density, total lipids, and total carbohydrates) on host immune activity, we ran a redundancy analysis (RDA) using the vegan package (v2.6.6)[127]. Before starting with this multivariate approach, we tested for and confirmed no collinearity among our continuous predictor variables (symbiont density, lipids, and carbohydrates). Outliers in all variables were removed (3 total), and all continuous variables were centered and scaled before separation into predictor (i.e., symbiont density, lipids, carbohydrates) and response (i.e., catalase, total phenoloxidase, and antibacterial activity, and melanin concentration) data frames. An RDA was used to identify which variables best-predicted variation in immunity across our samples. Immune parameters (catalase, TPO, melanin, and antibacterial activity) were input as response variables, with both continuous (symbiont density, energetic reserves) and fixed (temperature treatment, clonal line, immune challenge) variables used as predictors of interest. Initially, the RDA was run with all

possible predictor variables, excluding samples that had missing data in one or more response or predictor variables ($N = 41$). From there, we used forward selection to identify which predictor variables explained significant variation in our dataset. After identifying significant predictor variables, we ran a final RDA using the best-fit model determined by forward selection (~Treatment + Carbohydrates + Lipids).

Finally, we used linear modeling to assess variation in individual immune parameters with respect to the statistically relevant factors determined via RDA (treatment, carbohydrate, lipids). For normally distributed immune parameters (catalase, total phenoloxidase, antibacterial activity) we used GLMs. Global models with all possible additive and interactive variables were analyzed for catalase, total phenoloxidase, and antibacterial activity independently. All models were dredged and ranked via AICc using the MuMIn package (v1.47.5)[126], where applicable. Models with delta AICc values less than or equal to 2 were averaged to determine the best-fit models for each immune parameter. For melanin, which was right skewed with multiple zero measurements, we adopted a two-tiered strategy. First, we used a probit model (i.e., a generalized linear model with binomial error structure) to predict the presence of melanin among samples using heat treatment, carbohydrate, and lipid concentration as predictors. We then removed samples in which melanin concentration was below the limit of detection and used multiple regression to predict melanin concentrations employing the same predictors.

Reporting summary

Further information on research design is available in the Nature Portfolio Reporting Summary linked to this article.

Data availability

All raw data used in the described analyses is supplied as Supplementary Data 1.

Code availability

All R code used in the described analyses is supplied as Supplementary File 1.

Received: 4 November 2023; Accepted: 2 October 2024;
Published online: 15 October 2024

References

1. Rosenzweig, C. et al. Attributing physical and biological impacts to anthropogenic climate change. *Nature* **453**, 353–357 (2008).
2. Hansen, G. & Stone, D. Assessing the observed impact of anthropogenic climate change. *Nat. Clim. Change* **6**, 532–537 (2015).
3. Doney, S. C. et al. Climate change impacts on marine ecosystems. *Annu. Rev. Mar. Sci.* **4**, 11–37 (2011).
4. Scavia, D. et al. Climate change impacts on U.S. coastal and marine ecosystems. *Estuaries* **25**, 149–164 (2002).
5. Hoegh-Guldberg, O. & Bruno, J. F. The impact of climate change on the world's marine ecosystems. *Science* **328**, 1523–1528 (2010).
6. Smith, K. E. et al. Biological impacts of marine heatwaves. *Annu. Rev. Mar. Sci.* **15**, 119–145 (2023).
7. Genin, A., Levy, L., Sharon, G., Raitsos, D. E. & Diamant, A. Rapid onsets of warming events trigger mass mortality of coral reef fish. *Proc. Natl Acad. Sci. USA* **117**, 25378–25385 (2020).
8. Wild, S. et al. Long-term decline in survival and reproduction of dolphins following a marine heatwave. *Curr. Biol.* **29**, R239–R240 (2019).
9. Rivetti, I., Fraschetti, S., Lionello, P., Zambianchi, E. & Boero, F. Global warming and mass mortalities of benthic invertebrates in the Mediterranean Sea. *PLoS ONE* **9**, e115655 (2014).
10. Smale, D. A. Impacts of ocean warming on kelp forest ecosystems. *N. Phytol.* **225**, 1447–1454 (2020).
11. Bateman, K. S., Feist, S. W., Bignell, J. P., Bass, D. & Stentiford, G. D. in *Marine Disease Ecology* (Oxford University Press, 2020).
12. Sanderson, C. E. & Alexander, K. A. Unchartered waters: climate change likely to intensify infectious disease outbreaks causing mass mortality events in marine mammals. *Glob. Chang. Biol.* **26**, 4284–4301 (2020).
13. Patterson, K. R. Modelling the impact of disease-induced mortality in an exploited population: the outbreak of the fungal parasite (Ichthyophonus)(hoferi) in the North Sea herring (*Clupea harengus*). *Can. J. Fish. Aquat. Sci.* **53**, 2870–2887 (1996).
14. Hamilton, S. L. et al. Disease-driven mass mortality event leads to widespread extirpation and variable recovery potential of a marine predator across the eastern Pacific. *Proc. Biol. Sci.* **288**, 20211195 (2021).
15. Short, F. T., Muehlstein, L. K. & Porter, D. Eelgrass wasting disease: cause and recurrence of a marine epidemic. *Biol. Bull.* **173**, 557–562 (1987).
16. Adams, S. M. Assessing cause and effect of multiple stressors on marine systems. *Mar. Pollut. Bull.* **51**, 649–657 (2005).
17. Crain, C. M., Kroeker, K. & Halpern, B. S. Interactive and cumulative effects of multiple human stressors in marine systems. *Ecol. Lett.* **11**, 1304–1315 (2008).
18. Harvell, C. D. et al. Climate warming and disease risks for terrestrial and marine biota. *Science* **296**, 2158–2162 (2002).
19. Harvell, C. D. et al. Disease epidemic and a marine heat wave are associated with the continental-scale collapse of a pivotal predator (*Pycnopodia helianthoides*). *Sci. Adv.* https://doi.org/10.1126/sciadv.aau7042 (2019).
20. Olsen, Y. S. & Duarte, C. M. Combined effect of warming and infection by Labyrinthula sp. on the Mediterranean seagrass *Cymodocea nodosa*. *Mar. Ecol. Prog. Ser.* **532**, 101–109 (2015).
21. Ban, S. S., Graham, N. A. & Connolly, S. R. Evidence for multiple stressor interactions and effects on coral reefs. *Glob. Chang Biol.* **20**, 681–697 (2014).
22. Groner, M. L. et al. Warming sea surface temperatures fuel summer epidemics of eelgrass wasting disease. *Mar. Ecol. Prog. Ser.* **679**, 47–58 (2021).
23. Oliver, E. C. J. et al. The unprecedented 2015/16 Tasman Sea marine heatwave. *Nat. Commun.* **8**, 16101 (2017).
24. Miller, J. et al. Coral disease following massive bleaching in 2005 causes 60% decline in coral cover on reefs in the US Virgin Islands. *Coral Reefs* **28**, 925 (2009).
25. Croquer, A. & Weil, E. Changes in Caribbean coral disease prevalence after the 2005 bleaching event. *Dis. Aquat. Organ* **87**, 33–43 (2009).
26. Smith, S. V. & Buddemeier, R. W. Global change and coral reef ecosystems. *Annu. Rev. Ecol. Syst.* **23**, 89–118 (1992).
27. Gardner, T. A., Côté, I. M., Gill, J. A., Grant, A. & Watkinson, A. R. Long-term region-wide declines in Caribbean corals. *Science* **301**, 958–960 (2003).
28. Bruno, J. F. & Selig, E. R. Regional decline of coral cover in the Indo-Pacific: timing, extent, and subregional comparisons. *PLoS ONE* **2**, e711 (2007).
29. Brown, B. E. Coral bleaching: causes and consequences. *Coral Reefs* **16**, S129–S138 (1997).
30. Douglas, A. E. Coral bleaching—how and why? *Mar. Pollut. Bull.* **46**, 385–392 (2003).
31. Harvell, D. et al. Coral disease, environmental drivers, and the balance between coral and microbial associates. *Oceanography* **20**, 172–195 (2007).
32. Palmer, C. V. & Traylor-Knowles, N. G. in *Advances in Comparative Immunology* (eds Edwin L. Cooper & Edwin L. Cooper) 51–93 (2018).
33. Mydlarz, L. D., Fuess, L., Mann, W., Pinzón, J. H. & Gochfeld, D. J. Cnidarian Immunity: From Genomes to Phenomes. In *The Cnidaria, Past, Present and Future* (eds Goffredo, S. & Dubinsky, Z.) 441–466 (Springer, Cham, 2016) https://doi.org/10.1007/978-3-319-31305-4_28.

34. Parisi, M. G., Parrinello, D., Stabili, L. & Cammarata, M. Cnidarian immunity and the repertoire of defense mechanisms in anthozoans. *Biology (Basel)* **9**, 283 (2020).
35. Downs, C. A. et al. Oxidative stress and seasonal coral bleaching. *Free Radic. Biol. Med.* **33**, 533–543 (2002).
36. Wall, C. B. et al. The effects of environmental history and thermal stress on coral physiology and immunity. *Mar. Biol.* **165**, 56 (2018).
37. Johnston, M. A. et al. Coral bleaching and recovery from 2016 to 2017 at East and West Flower Garden Banks, Gulf of Mexico. *Coral Reefs* **38**, 787–799 (2019).
38. Winter, A., Appeldoorn, R., Bruckner, A., Williams, E. Jr. & Goenaga, C. Sea surface temperatures and coral reef bleaching off La Parguera, Puerto Rico (northeastern Caribbean Sea). *Coral Reefs* **17**, 377–382 (1998).
39. McClanahan, T. R., Ateweberhan, M., Muhando, C. A., Maina, J. & Mohammed, M. S. Effects of climate and seawater temperature variation on coral bleaching and mortality. *Ecol. Monogr.* **77**, 503–525 (2007).
40. Richardson, L. L., Goldberg, W. M., Carlton, R. G. & Halas, J. C. Coral disease outbreak in the Florida Keys: plague type II. *Rev. Biol. Trop.* **46**, 187–198 (1998).
41. Bruckner, A. W., Bruckner, R. J. & Williams, E. H. Jr Spread of a black-band disease epizootic through the coral reef system in St. Ann's Bay, Jamaica. *Bull. Mar. Sci.* **61**, 919–928 (1997).
42. Dahlgren, C., Pizarro, V., Sherman, K., Greene, W. & Oliver, J. Spatial and temporal patterns of stony coral tissue loss disease outbreaks in the Bahamas. *Front. Mar. Sci.* **8**, 682114 (2021).
43. Gil-Agudelo, D., Smith, G. & Weil, E. The white band disease type II pathogen in Puerto Rico. *Rev. Biol. Trop.* **54**, 59–67 (2006).
44. Brandt, M. E. & McManus, J. W. Disease incidence is related to bleaching extent in reef-building corals. *Ecology* **90**, 2859–2867 (2009).
45. Harvell, D., Kim, K., Quirolo, C., Weir, J. & Smith, G. Coral bleaching and disease: contributors to 1998 mass mortality in Briareum asbestinum (Octocorallia, Gorgonacea). *Hydrobiologia* **460**, 97–104 (2001).
46. Howells, E. J., Vaughan, G. O., Work, T. M., Burt, J. A. & Abrego, D. Annual outbreaks of coral disease coincide with extreme seasonal warming. *Coral Reefs* **39**, 771–781 (2020).
47. Burke, S. et al. The impact of rising temperatures on the prevalence of coral diseases and its predictability: a global meta-analysis. *Ecol. Lett.* **26**, 1466–1481 (2023).
48. Jones, N. P., Kabay, L., Semon Lunz, K. & Gilliam, D. S. Temperature stress and disease drives the extirpation of the threatened pillar coral, Dendrogyra cylindrus, in southeast Florida. *Sci. Rep.* **11**, 14113 (2021).
49. Miller, J., Waara, R., Muller, E. & Rogers, C. Coral bleaching and disease combine to cause extensive mortality on reefs in US Virgin Islands. *Coral Reefs* **25**, 418–418 (2006).
50. Zaragoza, W. J. et al. Outcomes of infections of sea anemone *Aiptasia pallida* with Vibrio spp. pathogenic to corals. *Micro Ecol.* **68**, 388–396 (2014).
51. Cervino, J. M. et al. Relationship of Vibrio species infection and elevated temperatures to yellow blotch/band disease in Caribbean corals. *Appl. Environ. Microbiol* **70**, 6855–6864 (2004).
52. Vidal-Dupiol, J. et al. Thermal stress triggers broad *Pocillopora damicornis* transcriptomic remodeling, while *Vibrio coralliilyticus* infection induces a more targeted immuno-suppression response. *PLoS ONE* **9**, e107672 (2014).
53. Palmer, C. V. Warmer water affects immunity of a tolerant reef coral. *Front. Mar. Sci.* **5**, 253 (2018).
54. Zhou, Z. et al. Suppression of NF-kappaB signal pathway by NLRC3-like protein in stony coral Acropora aculeus under heat stress. *Fish. Shellfish Immunol.* **67**, 322–330 (2017).
55. Bisanti, L. et al. How does warmer sea water change the sensitivity of a Mediterranean thermophilic coral after immune-stimulation? *Coral Reefs* **43**, 137–150 (2024).
56. Takagi, T., Yoshioka, Y., Zayasu, Y., Satoh, N. & Shinzato, C. Transcriptome analyses of immune system behaviors in primary polyp of coral *Acropora digitifera* exposed to the bacterial pathogen *Vibrio coralliilyticus* under thermal loading. *Mar. Biotechnol.* **22**, 748–759 (2020).
57. van de Water, J. et al. Antimicrobial and stress responses to increased temperature and bacterial pathogen challenge in the holobiont of a reef-building coral. *Mol. Ecol.* **27**, 1065–1080 (2018).
58. Eliachar, S. et al. Heat stress increases immune cell function in Hexacorallia. *Front. Immunol.* **13**, 1016097 (2022).
59. van de Water, J. A. J. M. et al. Elevated seawater temperatures have a limited impact on the coral immune response following physical damage. *Hydrobiologia* **759**, 201–214 (2015).
60. Tremblay, P., Naumann, M. S., Sikorski, S., Grover, R. & Ferrier-Pagès, C. Experimental assessment of organic carbon fluxes in the scleractinian coral *Stylophora pistillata* during a thermal and photo stress event. *Mar. Ecol. Prog. Ser.* **453**, 63–77 (2012).
61. Grottoli, A. G., Rodrigues, L. J. & Palardy, J. E. Heterotrophic plasticity and resilience in bleached corals. *Nature* **440**, 1186–1189 (2006).
62. Rodrigues, L. J. & Grottoli, A. G. Energy reserves and metabolism as indicators of coral recovery from bleaching. *Limnol. Oceanogr.* **52**, 1874–1882 (2007).
63. Ng'oma, E., Perinchery, A. M. & King, E. G. How to get the most bang for your buck: the evolution and physiology of nutrition-dependent resource allocation strategies. *Proc. R. Soc. B Biol. Sci.* **284**, 20170445 (2017).
64. Zera, A. J. & Harshman, L. G. The physiology of life history trade-offs in animals. *Annu. Rev. Ecol. Syst.* **32**, 95–126 (2001).
65. Garland, T., Downs, C. J. & Ives, A. R. Trade-offs (and constraints) in organismal biology. *Physiol. Biochem. Zool.* **95**, 82–112 (2022).
66. Rauw, W. M. Immune response from a resource allocation perspective. *Front. Genet.* **3**, 267 (2012).
67. Houston, A. I., McNamara, J. M., Barta, Z. & Klasing, K. C. The effect of energy reserves and food availability on optimal immune defence. *Proc. Biol. Sci.* **274**, 2835–2842 (2007).
68. McNamara, J. M. & Buchanan, K. L. Stress, resource allocation, and mortality. *Behav. Ecol.* **16**, 1008–1017 (2005).
69. Mansfield, K. M. & Gilmore, T. D. Innate immunity and cnidarian-Symbiodiniaceae mutualism. *Dev. Comp. Immunol.* **90**, 199–209 (2019).
70. Fuess, L. E., Palacio-Castro, A. M., Butler, C. C., Baker, A. C. & Mydlarz, L. D. Increased algal symbiont density reduces host immunity in a threatened caribbean coral species, *Orbicella faveolata*. *Front. Ecol. Evolut.* **8**, 572942 (2020).
71. Berthelier, J. et al. Implication of the host TGFβ pathway in the onset of symbiosis between larvae of the coral Fungia scutaria and the dinoflagellate Symbiodinium sp. (clade C1f). *Coral Reefs* **36**, 1263–1268 (2017).
72. Detournay, O., Schnitzler, C. E., Poole, A. & Weis, V. M. Regulation of cnidarian-dinoflagellate mutualisms: evidence that activation of a host TGFbeta innate immune pathway promotes tolerance of the symbiont. *Dev. Comp. Immunol.* **38**, 525–537 (2012).
73. Jacobovitz, M. R. et al. Dinoflagellate symbionts escape vomocytosis by host cell immune suppression. *Nat. Microbiol.* **6**, 769–782 (2021).
74. Weis, V. M., Davy, S. K., Hoegh-Guldberg, O., Rodriguez-Lanetty, M. & Pringle, J. R. Cell biology in model systems as the key to understanding corals. *Trends Ecol. Evol.* **23**, 369–376 (2008).
75. LaJeunesse, T. C. et al. Systematic revision of symbiodiniaceae highlights the antiquity and diversity of coral endosymbionts. *Curr. Biol.* **28**, 2570–2580.e2576 (2018).

76. Voolstra, C. R. A journey into the wild of the cnidarian model system Aiptasia and its symbionts. *Mol. Ecol.* **22**, 4366–4368 (2013).
77. Pirotta, E. et al. Understanding the combined effects of multiple stressors: a new perspective on a longstanding challenge. *Sci. Total Environ.* **821**, 153322 (2022).
78. Maor-Landaw, K. & Levy, O. in *The Cnidaria, Past, Present and Future: The world of Medusa and her sisters* (eds S. Goffredo & Z. Dubinsky) 523–543 (Springer International Publishing, 2016).
79. Weil, E., Weil-Allen, A. & Weil, A. Coral and cnidarian welfare in a changing sea. In *The Welfare of Invertebrate Animals. Animal Welfare* (eds Carere, C. & Mather, J.) vol 18, 123–145 (Springer, Cham, 2019) https://doi.org/10.1007/978-3-030-13947-6_6.
80. Muller, E. M., Bartels, E. & Baums, I. B. Bleaching causes loss of disease resistance within the threatened coral species *Acropora cervicornis*. *eLife* **7**, e35066 (2018).
81. Precht, W. F., Gintert, B. E., Robbart, M. L., Fura, R. & van Woesik, R. Unprecedented disease-related coral mortality in Southeastern Florida. *Sci. Rep.* **6**, 31374 (2016).
82. Palmer, C. V. et al. Patterns of coral ecological immunology: variation in the responses of Caribbean corals to elevated temperature and a pathogen elicitor. *J. Exp. Biol.* **214**, 4240–4249 (2011).
83. Traylor-Knowles, N. et al. Gene expression response to stony coral tissue loss disease transmission in *M. cavernosa* and *O. faveolata* from Florida. *Front. Mar. Sci.* https://doi.org/10.3389/fmars.2021.681563 (2021).
84. Huntley, N. et al. Experimental transmission of Stony Coral Tissue Loss Disease results in differential microbial responses within coral mucus and tissue. *ISME Commun.* **2**, 46 (2022).
85. Thornhill, D. J., Xiang, Y., Pettay, D. T., Zhong, M. & Santos, S. R. Population genetic data of a model symbiotic cnidarian system reveal remarkable symbiotic specificity and vectored introductions across ocean basins. *Mol. Ecol.* **22**, 4499–4515 (2013).
86. Vollmer, S. V. & Kline, D. I. Natural disease resistance in threatened staghorn corals. *PLoS ONE* **3**, e3718 (2008).
87. Miller, M. W. et al. Genotypic variation in disease susceptibility among cultured stocks of elkhorn and staghorn corals. *PeerJ* **7**, e6751 (2019).
88. Wright, R. M. et al. Intraspecific differences in molecular stress responses and coral pathobiome contribute to mortality under bacterial challenge in *Acropora millepora*. *Sci. Rep.* **7**, 1–13 (2017).
89. Brown, T. & Rodriguez-Lanetty, M. Defending against pathogens – immunological priming and its molecular basis in a sea anemone, cnidarian. *Sci. Rep.* **5**, 17425 (2015).
90. Seneca, F., Davtian, D., Boyer, L. & Czerucka, D. Gene expression kinetics of *Exaiptasia pallida* innate immune response to *Vibrio parahaemolyticus* infection. *BMC Genomics* **21**, 768 (2020).
91. Valadez-Ingersoll, M. et al. Starvation differentially affects gene expression, immunity and pathogen susceptibility across symbiotic states in a model cnidarian. *Proc. R. Soc. B* **291**, 20231685 (2024).
92. Changsut, I., Womack, H. R., Shickle, A., Sharp, K. H. & Fuess, L. E. Variation in symbiont density is linked to changes in constitutive immunity in the facultatively symbiotic coral, *Astrangia poculata*. *Biol. Lett.* **18**, 20220273 (2022).
93. Valadez-Ingersoll, M. et al. Nutrient deprivation differentially affects gene expression, immunity, and pathogen susceptibility across symbiotic states in a model cnidarian. *bioRxiv* https://doi.org/10.1101/2023.07.30.551141 (2023).
94. Jokiel, P. L. & Coles, S. L. Response of Hawaiian and other Indo-Pacific reef corals to elevated temperature. *Coral Reefs* **8**, 155–162 (1990).
95. Imbs, A. B. & Yakovleva, I. M. Dynamics of lipid and fatty acid composition of shallow-water corals under thermal stress: an experimental approach. *Coral Reefs* **31**, 41–53 (2011).
96. Ermolenko, E. V. & Sikorskaya, T. V. Lipidome of the reef-building coral Acropora cerealis: changes under thermal stress. *Biochem. Syst. Ecol.* https://doi.org/10.1016/j.bse.2021.104276 (2021).
97. Kochman, N. A.-R., Grover, R., Rottier, C., Ferrier-Pages, C. & Fine, M. The reef building coral *Stylophora pistillata* uses stored carbohydrates to maintain ATP levels under thermal stress. *Coral Reefs* **40**, 1473–1485 (2021).
98. Tortorelli, G., Belderok, R., Davy, S. K., McFadden, G. I. & van Oppen, M. J. H. Host genotypic effect on algal symbiosis establishment in the coral model, the anemone *Exaiptasia diaphana*, from the Great Barrier Reef. *Front. Mar. Sci.* **6**, 833 (2020).
99. Krueger, T. et al. Differential coral bleaching—contrasting the activity and response of enzymatic antioxidants in symbiotic partners under thermal stress. *Comp. Biochem. Physiol. Part A* **190**, 15–25 (2015).
100. Wall, C. B. et al. Shifting baselines: Physiological legacies contribute to the response of reef corals to frequent heatwaves. *Funct. Ecol.* **35**, 1366–1378 (2021).
101. Mydlarz, L. D., Couch, C. S., Weil, E., Smith, G. & Harvell, C. D. Immune defenses of healthy, bleached and diseased Montastraea faveolata during a natural bleaching event. *Dis. Aquat. Org.* **87**, 67–78 (2009).
102. Baruah, K., Norouzitallab, P., Linayati, L., Sorgeloos, P. & Bossier, P. Reactive oxygen species generated by a heat shock protein (Hsp) inducing product contributes to Hsp70 production and Hsp70-mediated protective immunity in Artemia franciscana against pathogenic vibrios. *Dev. Comp. Immunol.* **46**, 470–479 (2014).
103. Baruah, K., Ranjan, J., Sorgeloos, P., Macrae, T. H. & Bossier, P. Priming the prophenoloxidase system of Artemia franciscana by heat shock proteins protects against Vibrio campbellii challenge. *Fish. Shellfish Immunol.* **31**, 134–141 (2011).
104. Anthony, K. R. N., Connolly, S. R. & Hoegh-Guldberg, O. Bleaching, energetics, and coral mortality risk: effects of temperature, light, and sediment regime. *Limnol. Oceanogr.* **52**, 716–726 (2007).
105. Ferrier-Pagès, C., Rottier, C., Beraud, E. & Levy, O. Experimental assessment of the feeding effort of three scleractinian coral species during a thermal stress: effect on the rates of photosynthesis. *J. Exp. Mar. Biol. Ecol.* **390**, 118–124 (2010).
106. Tremblay, P., Gori, A., Maguer, J. F., Hoogenboom, M. & Ferrier-Pages, C. Heterotrophy promotes the re-establishment of photosynthate translocation in a symbiotic coral after heat stress. *Sci. Rep.* **6**, 38112 (2016).
107. Anthony, K. R. N., Hoogenboom, M. O., Maynard, J. A., Grottoli, A. G. & Middlebrook, R. Energetics approach to predicting mortality risk from environmental stress: a case study of coral bleaching. *Funct. Ecol.* **23**, 539–550 (2009).
108. Kenkel, C. D., Meyer, E. & Matz, M. V. Gene expression under chronic heat stress in populations of the mustard hill coral (*Porites astreoides*) from different thermal environments. *Mol. Ecol.* **22**, 4322–4334 (2013).
109. Paradis, B. T., Henry, R. P. & Chadwick, N. E. Compound effects of thermal stress and tissue abrasion on photosynthesis and respiration in the reef-building coral Acropora cervicornis (Lamarck, 1816). *J. Exp. Mar. Biol. Ecol.* https://doi.org/10.1016/j.jembe.2019.151222 (2019).
110. Brunner, F. S., Schmid-Hempel, P. & Barribeau, S. M. Protein-poor diet reduces host-specific immune gene expression in *Bombus terrestris*. *Proc. Biol. Sci*. https://doi.org/10.1098/rspb.2014.0128 (2014).
111. Bellis, E. S. & Denver, D. R. Natural variation in responses to acute heat and cold stress in a sea anemone model system for coral bleaching. *Biol. Bull.* **233**, 168–181 (2017).
112. Cleves, P. A., Krediet, C. J., Lehnert, E. M., Onishi, M. & Pringle, J. R. Insights into coral bleaching under heat stress from analysis of gene

expression in a sea anemone model system. *Proc. Natl Acad. Sci. USA* **117**, 28906–28917 (2020).
113. Ben-Haim, Y. et al. *Vibrio coralliilyticus* sp. nov., a temperature-dependent pathogen of the coral *Pocillopora damicornis*. *Int. J. Syst. Evolut. Microbiol.* **53**, 309–315 (2003).
114. Bateman, T. G. *Physiological Dynamics of Cnidarian-Dinoflagellate Symbioses Under Climate Change*, (University of Delaware, 2022).
115. Pinzón, C., Beach-Letendre, J. H., Weil, J. & Mydlarz, E. L. D. Relationship between phylogeny and immunity suggests older Caribbean coral lineages are more resistant to disease. *PLoS ONE* **9**, e104787 (2014).
116. Mydlarz, L. D. & Palmer, C. V. The presence of multiple phenoloxidases in Caribbean reef-building corals. *Comp. Biochem. Physiol. Part A* **159**, 372–378 (2011).
117. Lesser, M. P. Using energetic budgets to assess the effects of environmental stress on corals: are we measuring the right things? *Coral Reefs* **32**, 25–33 (2013).
118. Fitt, W. K., McFarland, F. K., Warner, M. E. & Chilcoat, G. C. Seasonal patterns of tissue biomass and densities of symbiotic dinoflagellates in reef corals and relation to coral bleaching. *Limnol. Oceanogr.* **45**, 677–685 (2000).
119. Cheng, Y.-S., Zheng, Y. & VanderGheynst, J. S. Rapid quantitative analysis of lipids using a colorimetric method in a microplate format. *Lipids* **46**, 95–103 (2011).
120. Masuko, T. et al. Carbohydrate analysis by a phenol-sulfuric acid method in microplate format. *Anal. Biochem.* **339**, 69–72 (2005).
121. R: A language and environment for statistical computing (R Foundation for Statistical Computing, Vienna, Austria, 2021).
122. Millard, S. P. *EnvStats: An R Package for Environmental Statistics*. (Springer, 2013).
123. A Package for Survival Analysis in R (2024).
124. Johnson, L. L. & Shih, J. H. in *Principles and Practice of Clinical Research* 273–282 (2007).
125. Christensen, E. Multivariate survival analysis using Cox's regression model. *Hepatology* **7**, 1346–1358 (1987).
126. MuMIn: Multi-Model Inference (2023).
127. Oksanen, J. et al. vegan. *Community Ecology Package* (2024).

Acknowledgements

We would like to thank Sam Bedgood and Virginia Weis for providing anemone stock populations as well as Tim Bateman for sharing Aiptasia protocols. Additionally, we would like to thank Dr. Benjamin Martin and the Rhodes Lab at Texas State University for equipment usage. Finally, we would like to acknowledge members of the Texas State EEB discussion group for experimental assistance and data/paper feedback, respectively. In particular, we thank Chris Nice and Jim Fordyce for their contributions to the statistical analyses presented. Funding was provided by Texas State University (startup funding to L.E.F.), the National Science Foundation (PRFB 2209205 to E.M.B.), and the National Academies Gulf Research Program (early career fellowship to L.E.F.).

Author contributions

L.E.F. and S.C.D.V. conceptualized and designed the experiment. S.C.D.V., E.M.B., and P.Y.A. ran experiments. S.C.D.V. and P.Y.A. processed and analyzed all samples. L.E.F., E.M.B., and S.C.D.V. processed data and ran statistical analyses. All authors contributed to the paper writing and editing process.

Competing interests

The authors declare no competing interests.

Additional information

Supplementary information The online version contains supplementary material available at https://doi.org/10.1038/s42003-024-07005-8.

Correspondence and requests for materials should be addressed to Lauren E. Fuess.

Peer review information *Communications Biology* thanks Carolina Madeira, and the other, anonymous, reviewers for their contribution to the peer review of this work. Primary Handling Editors: Linn Hoffmann and David Favero.